SUPPORTING INFORMATION

## Dissociation of HNO$_3$ in Water Revisited : Experiment and Theory

Ipek Munar‡, Melike Özkan Özer≠, Edoardo Fusco#, Deniz Uner≠*, Viktorya Aviyente‡*, Michael Bühl#*

‡ Chemistry Department, Bogazici University, 34342 Bebek, Istanbul, Turkey
#EaStCHEM School of Chemistry, Biomedical Sciences Research Complex, and Centre of Magnetic Resonance, University of St Andrews, St Andrews KY16 9ST, U.K.
≠Middle East Technical University, Chemical Engineering, 06800 Ankara, Turkey
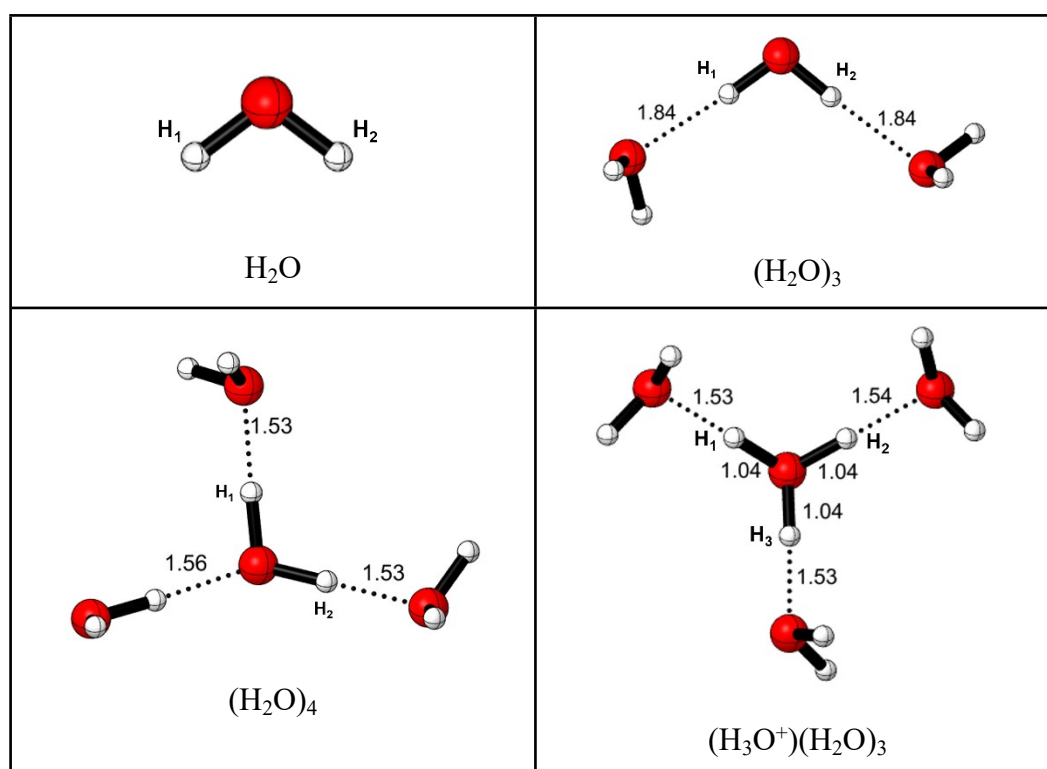
**Figure S1**. Structures of pure water clusters and solvated hydronium ion (optimised at PBE/6-311+G(2d,p), SMD=H$_2$O)
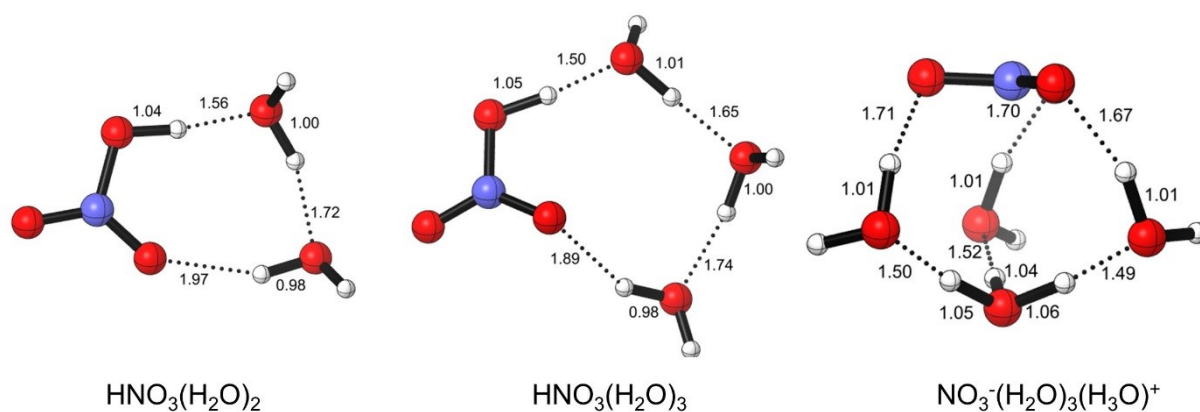
Figure S2. Structures of $HNO_3(H_2O)_n$ (n=2,3), $NO_3^-(H_2O)_3(H_3O)^+$ clusters (PBE/6-311+G(2d,p), gas phase)

Table S1. Electronic Energy (Zero Point Energies included) (Hartree) of $HNO_3(H_2O)_n$ (n=1,2), $NO_3^-(H_2O)_m(H_3O)^+$ (m=2-7) clusters (PBE/6-311+G(2d,p), 323.15K, SMD=H_2O)

	Formula	Electronic Energies
1	$HNO_3(H_2O)$	-357.086
2	$NO_3^-(H_2O)(H_3O)^+$	-433.4581
3	$NO_3^-(H_2O)_2(H_3O)^+$	-509.833
4	$NO_3^-(H_2O)_3(H_3O)^+$	-586.2066
5	$NO_3^-(H_2O)_4(H_3O)^+$	-662.5797
6	$NO_3^-(H_2O)_5(H_3O)^+$	-738.9519
7	$NO_3^-(H_2O)_6(H_3O)^+$	-815.3238
8	$NO_3^-(H_2O)_7(H_3O)^+$	-891.6943

Table S2. Calculated enthalpy of mixing values (kcal/mol) of $HNO_3(H_2O)_n$ (n=1-8) clusters compared with isothermal experimental heat of mixing (kcal/mol) (PBE/6-311+G(2d,p), 323.15K, SMD=H_2O)

Clusters	Mole Fraction	Enthalpy of mixing (calc.)	Heat of mixing (exp.)
$HNO_3(H_2O)$	0.50	-4.14	-2.17
$HNO_3(H_2O)_2$	0.33	-6.05	-3.02
$HNO_3(H_2O)_3$	0.25	-9.20	-3.39
$HNO_3(H_2O)_4$	0.20	-11.17	-4.03
$HNO_3(H_2O)_5$	0.17	-13.23	-4.18
$HNO_3(H_2O)_6$	0.14	-14.58	-4.16
$HNO_3(H_2O)_7$	0.13	-15.58	-4.38
$HNO_3(H_2O)_8$	0.11	-15.86	-4.20
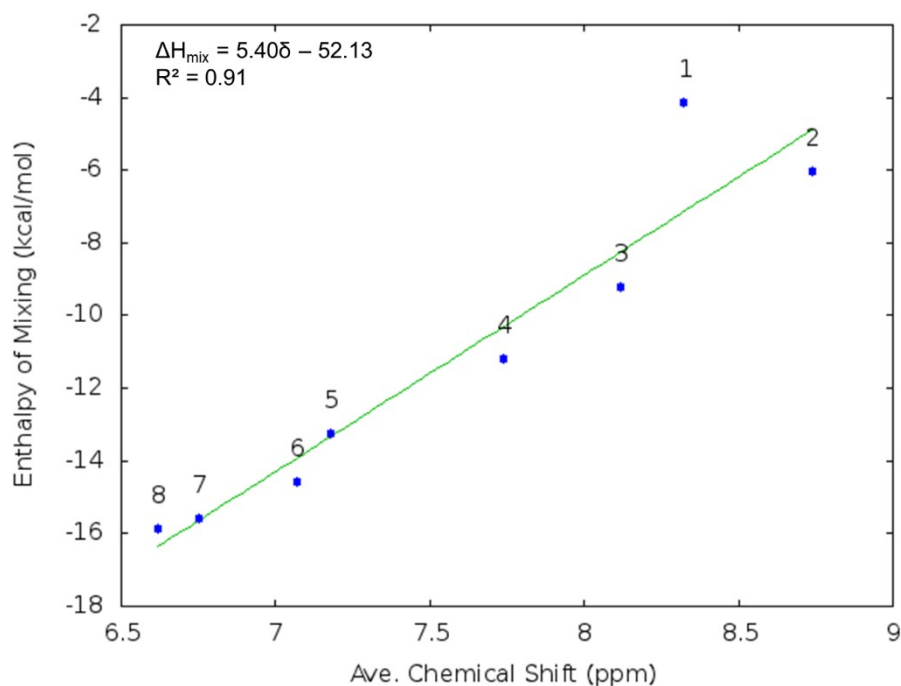
Figure S3. Enthalpy of mixing (kcal/mol) vs. Average Chemical Shift (ppm) (PBE/6-311+G(2d,p), 323.15K, SMD=H_2O, TMS= 31.38)
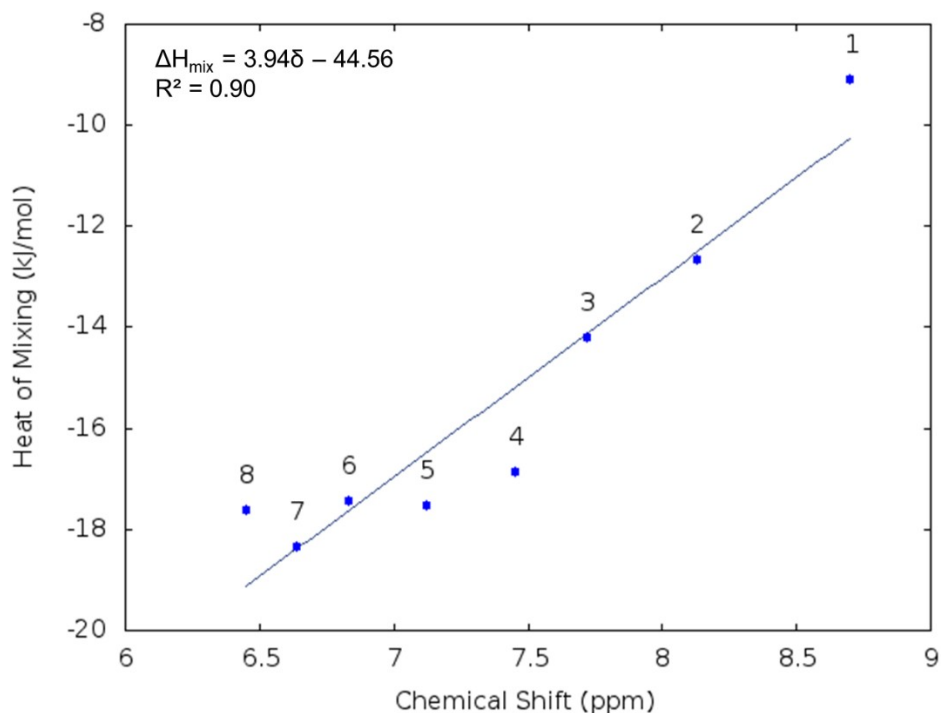
Figure S4. Heat of mixing (kJ/mol) vs. Chemical Shift (ppm)
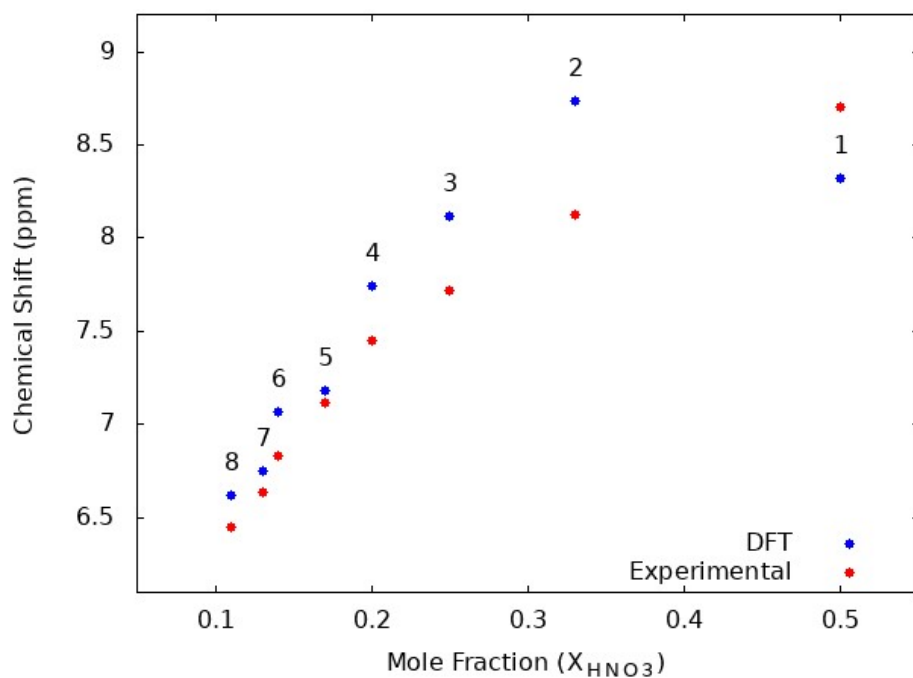
Figure S5. Calculated Average Chemical Shift (ppm) and Experimental Chemical Shift (ppm) vs Mole fraction (PBE/6-311+G(2d,p), 323.15K, SMD=H_2O, TMS= 31.38)

Magnetic properties calculation with periodic boundry conditions

To perform magnetic properties with periodic boundry conditions we started from a model system containing only a single water molecule (see Figure S6).
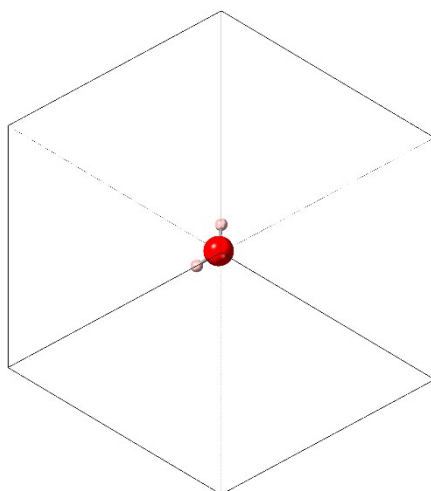
Figure S6. Unit cell for a single water molecule.

After geometry optimisation, we computed the chemical shielding as a function of the energy cut-off. We screened 11 cut-off values, ranging from 20 Ry to 120 Ry in 10 Ry steps. We found that a cut-off value of 60 Ry offers the best comprise between computational cost and accuracy, as the predicted chemical shift does not change when increasing the number of plane waves up to 120 Ry (see Table S3).

Table S3. Chemical shielding as a function of the cut-off value for the single water model (using a k-spacing of 0.04 Å^{-1}). Bold value selected for subsequent calculations.

| Cut-off (Ry)	^{1}H σ(ppm)
20	33.7
30	31.3
40	31.1
50	31.1
60	**31.2**
70	31.2
80	31.2
90	31.2
100	31.2
110	31.2
120	**31.2**

The second parameter we optimised is the k-spacing. We screened eight different k-spacing values and found that a spacing of 0.1 Å is satisfactory.

Table S4. Chemical shielding and its k-point spacing for the single water model. Bold value selected for subsequent calculations.

k-spacing ($Å^{-1}$)	^1H δ(ppm)
0.03	31.2
0.04	31.2
0.05	31.2
0.06	31.2
0.07	31.2
0.08	31.2
0.09	31.2
0.1	**31.2**

After performing MD simulations, the statistical stability of the predicted chemical shielding was evaluated through the cumulative average. It appears that ~200 points are sufficient to have a fully chemical shielding.
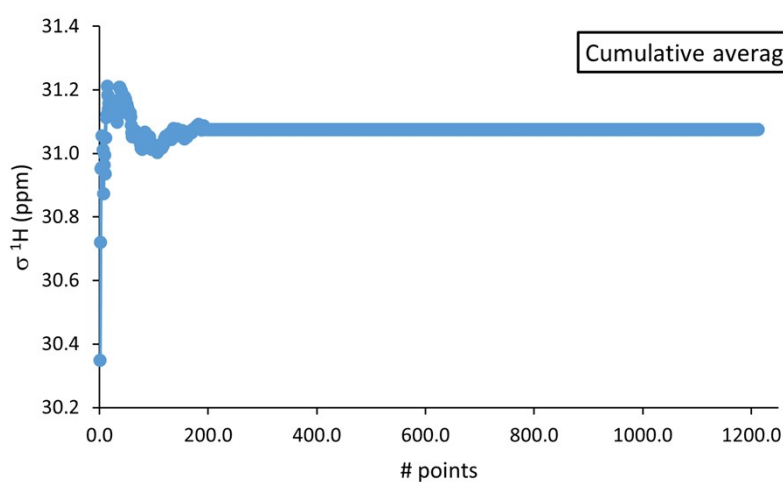

Figure S7. Cumulative average of the ^1H chemical shielding for the single water system.

Nitric acid solutions at 300 K

At 300 K it is immediate to see some differences among the different oxygen-oxygen radial distribution functions, $g_{OO(r)}$, systems (Figure 4 in the main text). The pure water has an intense peak close to 3 Å, which corresponds to the first coordination sphere. This peak is strongly shifted once the nitric acid is added to the solution, changing from 2.75 to 2.15 Å. It must be noted that both the $x = 0.19$ and $x = 0.50$ solution have the maximum in the same position and the only difference is its intensity. Interestingly, the more structured solution is the $x = 0.50$ one, suggesting that the interaction between water and nitric acid is strong as it "freezes" the molecules in place due to the hydrogen bonding network. A similar conclusion can be drawn for the pure water system as the height of first maximum is significantly more intense than the experimental one (Figure 5). The second maximum is more conserved among all system, both in terms of position and intensity, although only the pure water system has it significantly marked.

Regarding the $g_{OH}(r)$, this value is interesting as it informs on the proton movement in solution.
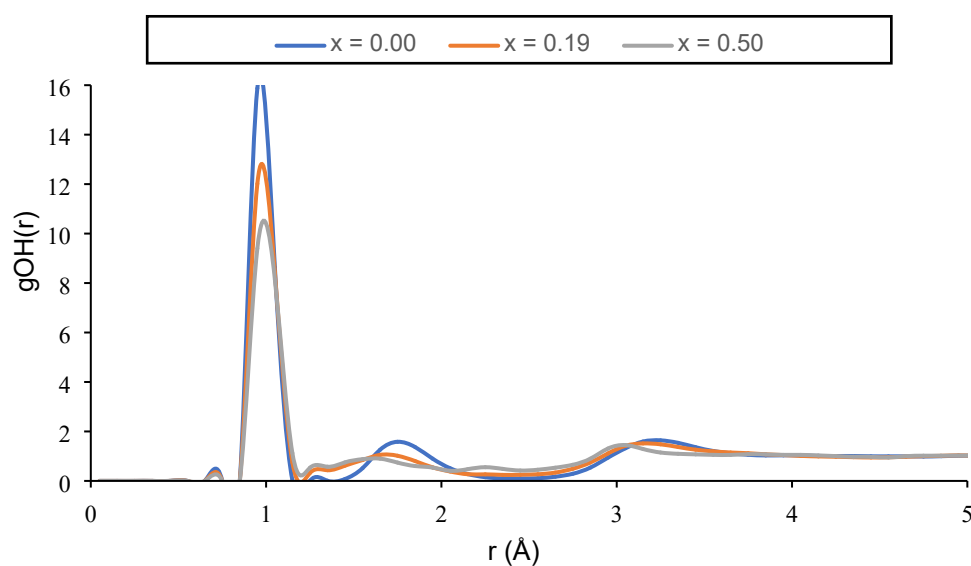
Figure S8. The oxygen-hydrogen RDF for the different systems computed at 300 K.

From Figure S8 it is evident how strong the hydrogen-oxygen interaction is. In fact, the first maximum dwarfs all the others, showcasing the localised nature of the protons. Looking at the pure water system, it appears that the highest peak corresponds to the covalently bound protons, while the second peak is associated with the hydrogen bonding to a nearby water molecule. The

last peak over 3 Å comes from the distance between the oxygen atom and the furthest hydrogen atom of a nearby water molecule (see Figure S9).
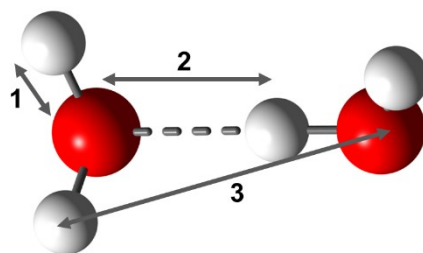

Figure S9. Key distances in the oxygen-hydrogen RDF plot, numbered and ordered according to their length.

Supplementary structural information can be obtained by deconvoluting the oxygen-hydrogen RDF into the water and nitric acid contribution. In particular, the integral of the deconvoluted RDF would provide a qualitative measure of the number of protons directly bonded to the first coordination sphere. The expected value for water is two while it is one for the nitric acid. If the integral over the radial distribution function is larger than the expected value some degree of proton exchanging is happening. In fact, if the integral predicts a value larger than the expected one, it means that one extra proton is interacting with the first coordination sphere of the oxygen. On the other hand, if the value is smaller, the oxygen-hydrogen bond is dissociating. It should be pointed out that the increase/decrease is a fractional number as the RDF is computed over the whole trajectory and associating/dissociating events will fluctuate in time. For the integral to increase by a whole unit a new stable bond must be formed with an extra proton. However, this is not the case for our system, where protonation/deprotonation events are in equilibrium and therefore only produce a fractional change to the integral over the oxygen-hydrogen RDF.

A)
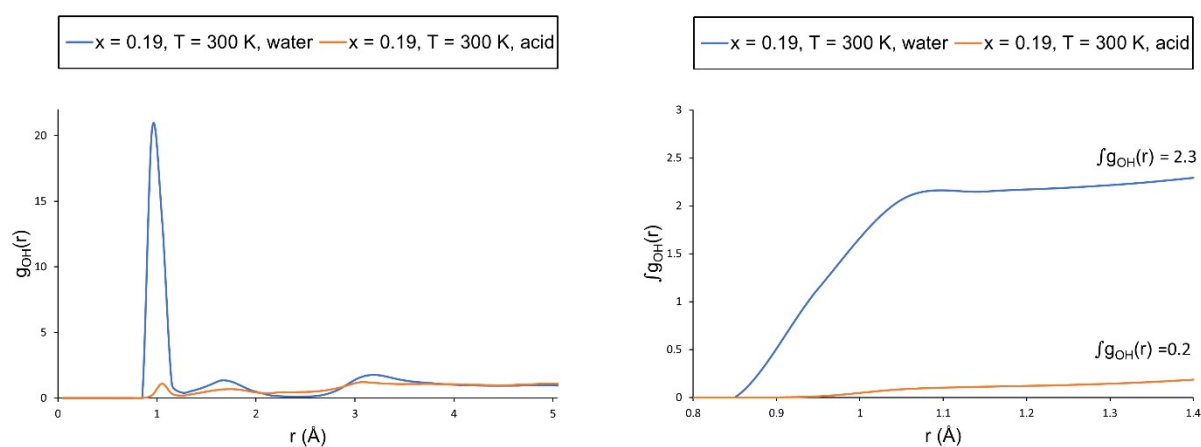
B)
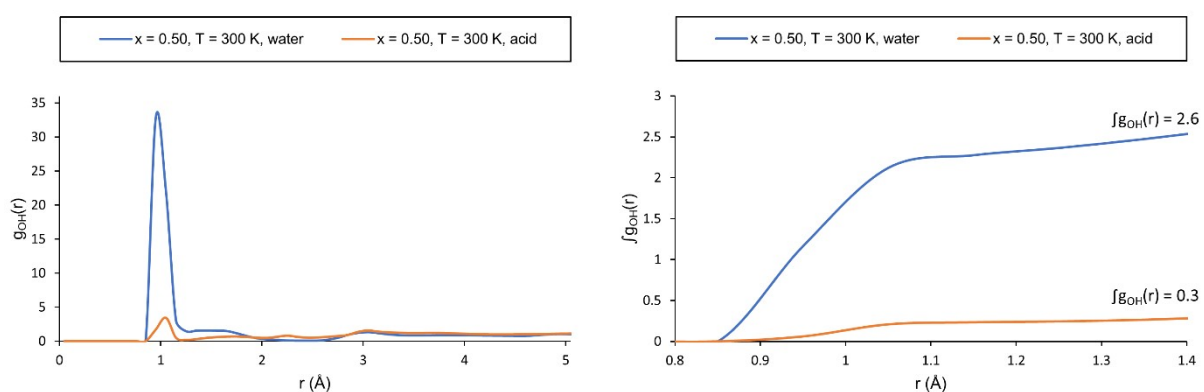
Figure S10. Left: the deconvoluted oxygen-hydrogen RDFs at 300 K. The legends "water" and "acid" refer to O atoms from water molecules and NO_3 moieties, respectively. right: integral $\int g_{OH}(r)4\pi r^2 dr$ of the deconvoluted oxygen-hydrogen RDF plotted up to the radius of the first coordination sphere. A: plots for x = 0.19, B: plots for x = 0.50.

Looking at Figure S10 and in particular at the integrals of the curves on the right-hand side, it is easy to see how the integral deviates from the expected value for pure water and pure nitric acid. To be more specific, the integral involving the water O atoms suggests the interaction with a third proton, forming H_3O^+, whereas the nitric acid dissociates the proton to form NO_3^-. We can find a difference based on the molar fraction as the integral for the water only solution (x = 0.50) increases to 2.6. This is most likely due to the larger amount of acid in the unit cell, which translates in more protons being dissociated and therefore more H_3O^+ species generated.

Table S6. Predicted and experimental chemical ^{1}H shifts for the three nitric acid solution with molecular fraction of 0.00, 0.19 and 0.50. The last column reports the difference between the two. All the data are reported in ppm and referred to the x=0.00 solution.

| x	δ(CASTEP, 300K)	δ(Exp., 300K)	Δδ
0.00	0.0	0.0	0.0
0.19	2.1	2.6	-0.5
0.50	4.3	4.0	0.3

Nitric acid solutions at 450 K

The oxygen-oxygen RDF of the pure water system shown in the main text (see Figure 5) displayed a significant difference between 300 and 450 K. The same cannot be said for the nitric acid solutions, for which minimal changes are found. The x =0.19 solutions shows a less structured behaviour as both peaks in the RDF are less intense at the higher temperature. Moreover, the second peak is significantly less structured suggesting that outside the first coordination sphere molecules have larger mobility (see left panel of Figure S11). The x=0.50 structure does not display a similar trend, as the peak intensity is found to be larger at the higher temperature, however the ratio between the first and second peak is unchanged (see right panel of Figure S11).

A)
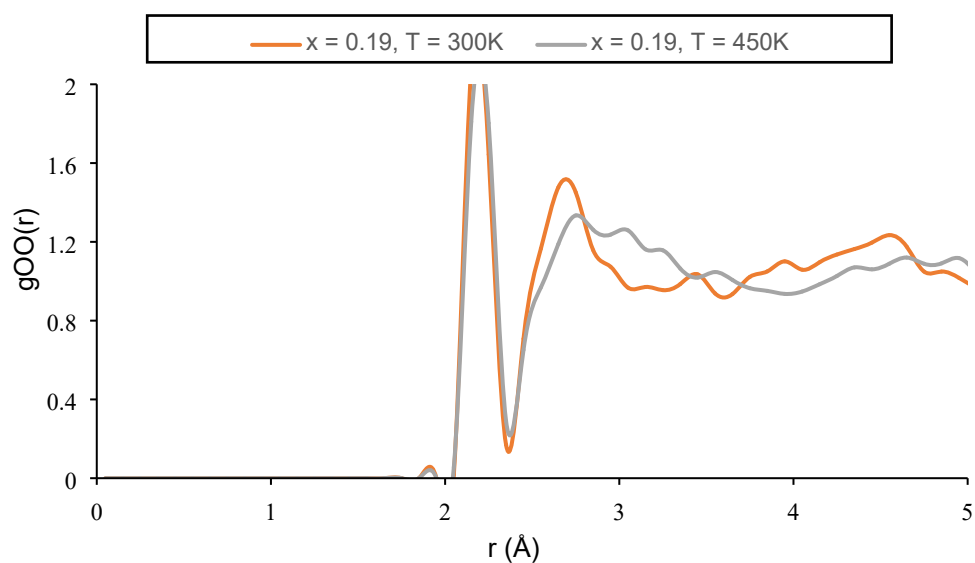
B)
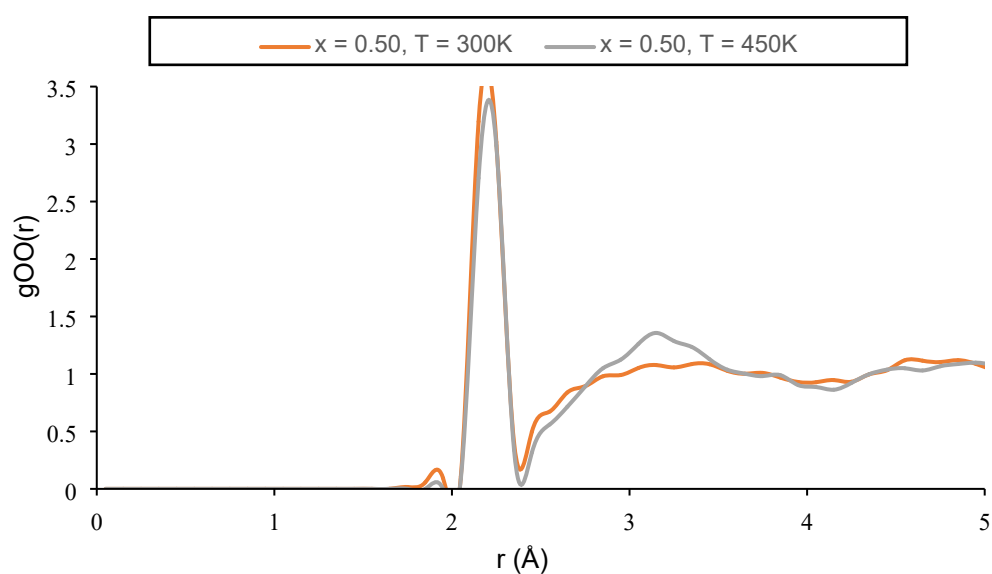
Figure S11. A: comparison of the oxygen-oxygen RDF for the x = 0.19 solution at 300 and 450 K. B: comparison of the oxygen-oxygen RDF for the x = 0.50 solution at 300 and 450 K

Looking at oxygen-hydrogen RDF of the pure water and of the other solutions, x = 0.19 and x = 0.50, it is immediately clear that the change is not marked. The first coordination sphere (first peak) is unaltered by the higher simulation temperature and this is not unexpected. In fact, as shown in Figure S9, this peak corresponds to the covalently bound proton to the oxygen which is not impacted by temperature.
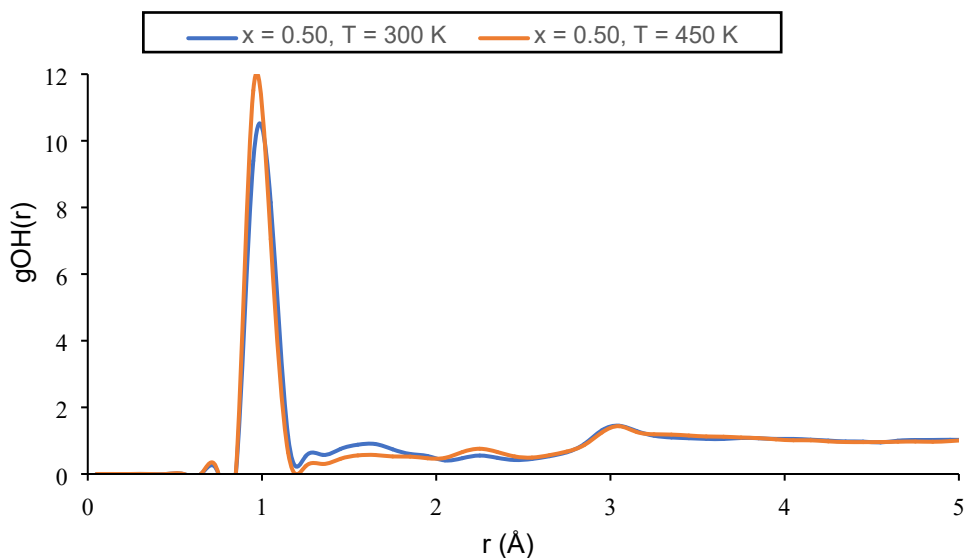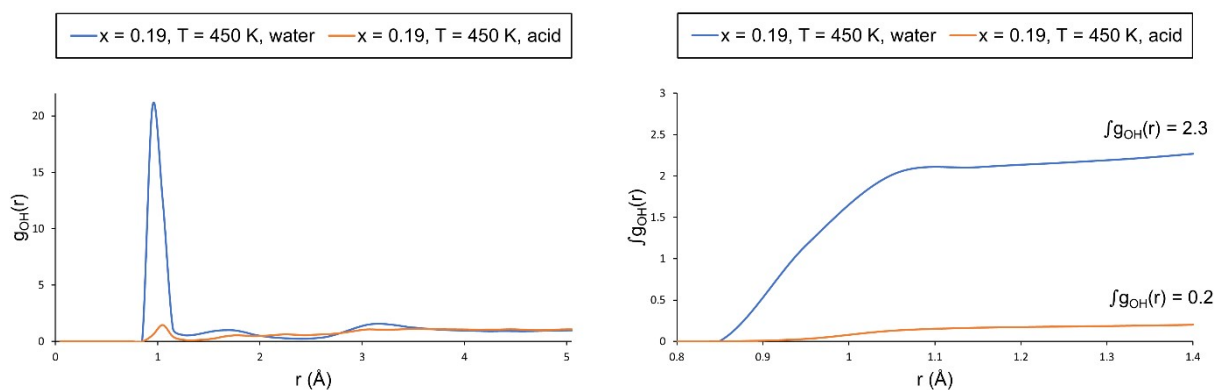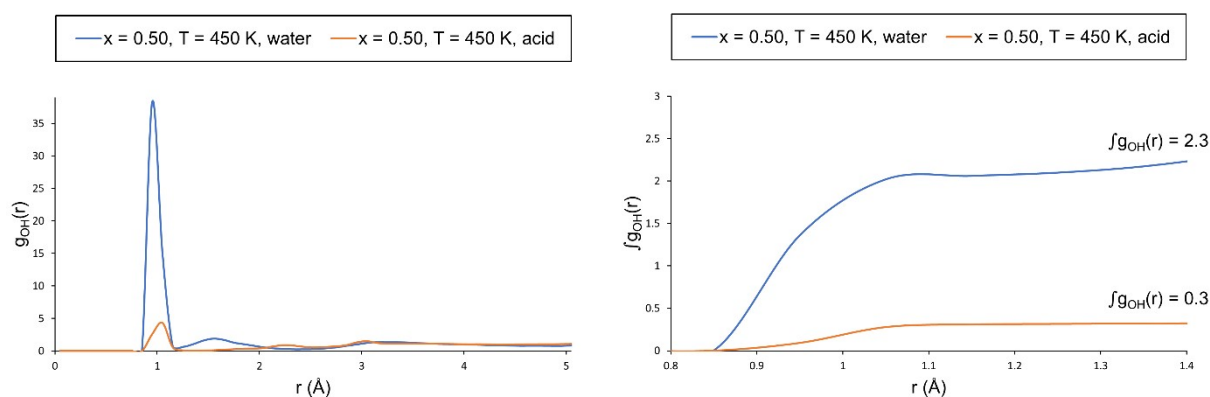
A)
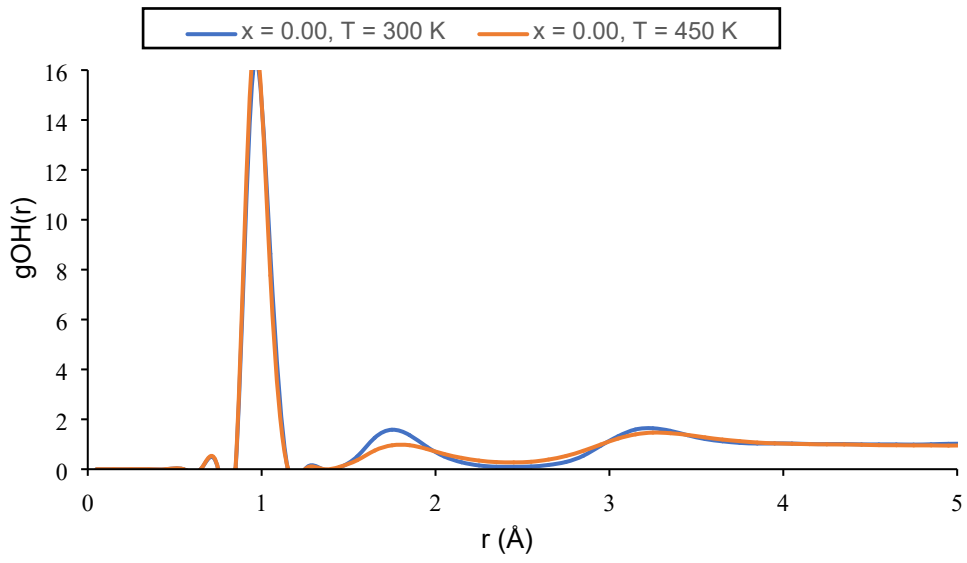
B)
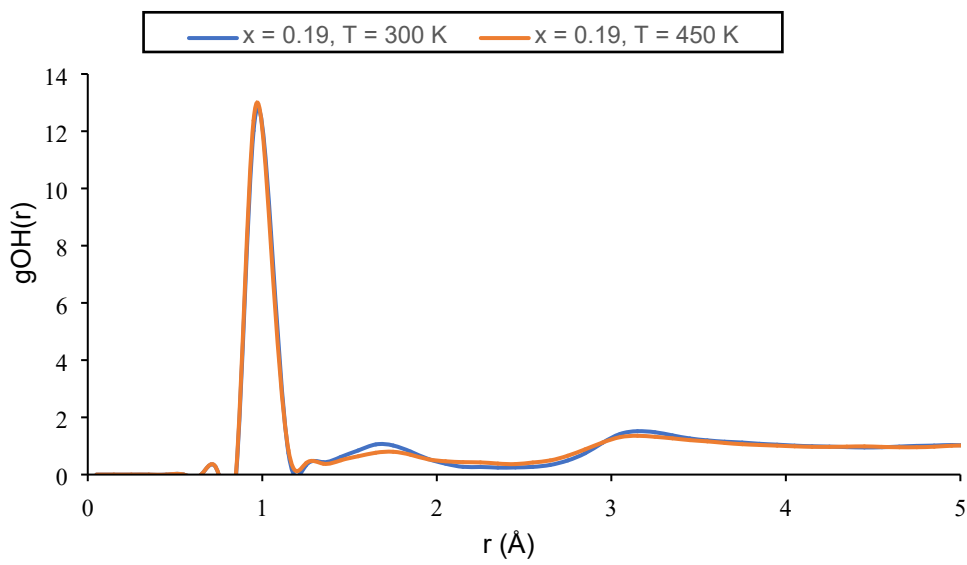
C)

Figure S12. The oxygen-hydrogen RDF for the three systems (A: x= 0.00; B: x = 0.19; C: x = 0.50) computed at 300 and 450 K.

Following our analysis for the 300 K simulation, we can deconvolute the oxygen-hydrogen RDF into individual components and account for protonation/deprotonation events in solution through the integral of the curve.

A)

B)

Figure S13. Left: the deconvoluted oxygen-hydrogen RDFs at 450 K. The legends "water" and "acid" refer to O atoms from water molecules and NO_3 moieties, respectively. right: integral $\int g_{OH}(r)4\pi r^2 dr$ of the deconvoluted oxygen-hydrogen RDF plotted up to the radius of the first coordination sphere. A: plots for x = 0.19, B: plots for x = 0.50

Inspecting the integral of the RDF for the x = 0.19 solution, it appears that temperature does not impact the amount of H_3O^+ and NO_3^- species generated. The same cannot be said for the x = 0.50 solution, for which the integral for the water-only solution drops from 2.6 to 2.3. The reason for this could be the increased mobility, as the H_3O^+ species has a shorter lifetime and dissociates with a faster rate with the higher temperature. This interpretation finds support in the oxygen-hydrogen RDF as the second peak is now larger, which suggests that the protons are found at a longer distance from the oxygen nucleus, as it would be expected for a more frequent dissociation process.
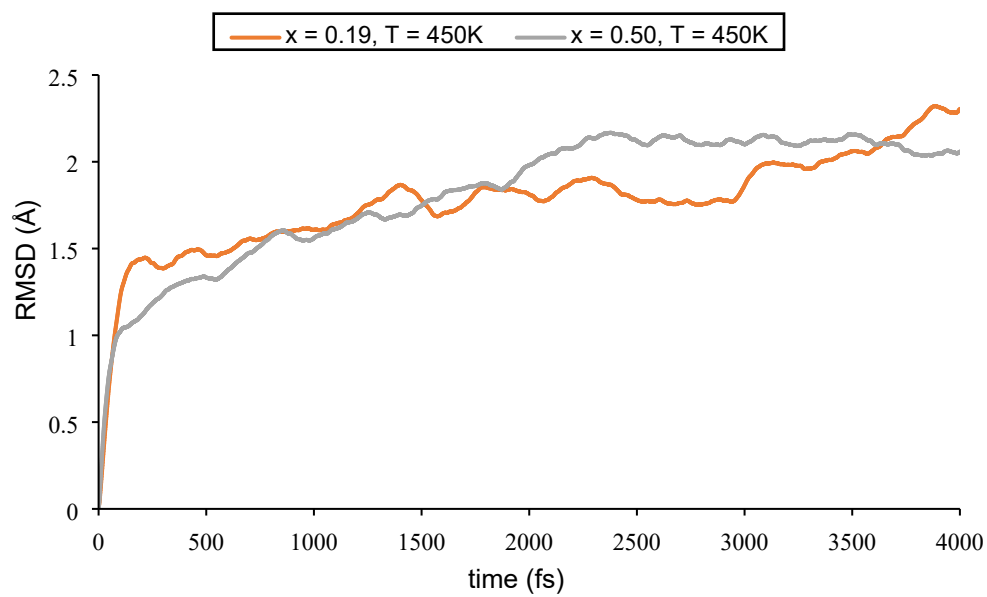
Figure S14 Plot of the RMSD for the x = 0.19 and x = 0.50 solutions at 450 K.
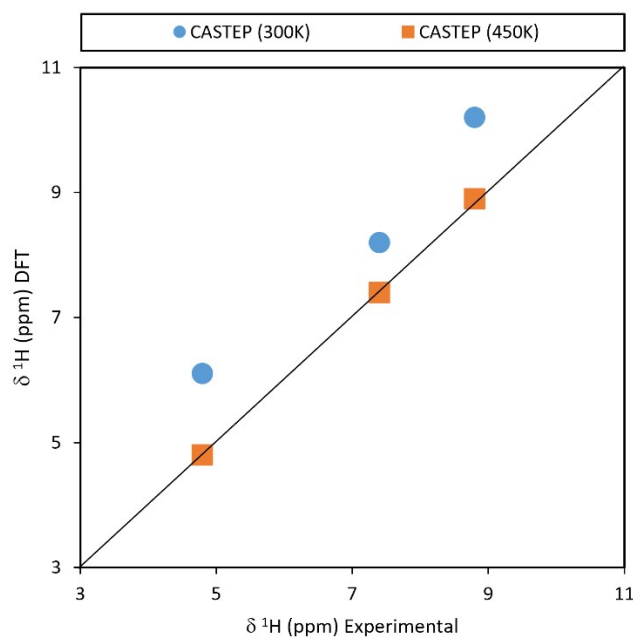
Figure S15 . Plot of the predicted against the experimental ^1H chemical shift at 300 and 450 K.

Cartesian Coordinates

(PBE/6-311+G(2d,p), SMD=H_2O)

$HNO_3(H_2O)$
N 0.86240600 0.05728900 -0.00024400
O 2.03668500 -0.29757900 0.02724900
O 0.44374100 1.21539700 -0.01080700
O -0.04988500 -0.95753100 -0.02046500
H -1.01706700 -0.51086000 -0.03525700
O -2.39348800 0.00449500 -0.09326600
H -2.36501000 0.90104400 0.29349600
H -2.95119300 -0.50946500 0.52179000

$NO_3^-(H_2O)(H_3O)^+$
N -1.30763600 -0.08257200 0.00186700
O -2.55213700 -0.17957500 0.03106400
O -0.56992700 -1.10587600 -0.02505700
O -0.78346100 1.10169900 -0.00223300
H 0.66074400 1.19237200 -0.03318100
O 1.72094400 1.31582900 -0.09747700
H 2.09050300 0.31407600 -0.04829900
H 2.01067200 1.77723200 0.71585300
O 2.24463800 -1.12766200 -0.08243700
H 1.27426000 -1.30945600 0.00378700
H 2.63681700 -1.43154800 0.75788500

$NO_3^-(H_2O)_2(H_3O)^+$
N -1.75451300 -0.00199000 0.02202900
O -3.00737000 0.01803400 0.06941400
O -1.12410000 0.89773800 -0.62493500
O -1.10749100 -0.92435100 0.62158200
H 3.28761100 -0.17210400 0.92119700
O 1.26351100 1.87331500 0.25138300
H 1.47157800 2.55142900 -0.41866900
H 0.40145100 1.46495100 -0.05372100
O 1.22157700 -1.81106700 -0.44490300
H 0.36721300 -1.45822800 -0.05447900
H 1.41397400 -2.62694800 0.05444900
O 2.87066800 -0.02015100 0.04967100
H 2.21533500 0.83541500 0.15147200
H 2.19006700 -0.84873200 -0.13215000

$NO_3^-(H_2O)_3(H_3O)^+$
N -1.51134600 0.02632800 -0.00375000
O -1.53815800 -0.91611100 0.84629600
O -1.47596500 1.23207200 0.38880700
O -1.50656400 -0.23811600 -1.24454300
O 0.96536300 2.24020200 -0.57305200

O 0.91869700 -1.53994900 -1.75774700
O 0.89102200 -0.63879500 2.21666200
H -0.03971700 -0.76824000 1.90004500
H 1.18001100 -1.52688800 2.49900900
H 0.94870600 -2.46698500 -1.45537200
H -0.02687800 -1.26724300 -1.64123900
H 1.26998600 2.91981500 0.05728100
H 0.03119700 2.04996500 -0.30294000
O 2.03754600 -0.02457100 -0.00276800
H 1.61996200 -0.66866100 -0.70870900
H 1.64902600 0.91985300 -0.22237000
H 1.61160500 -0.29376100 0.91130600

$NO_3^-(H_2O)_4(H_3O)^+$
N 1.42152900 0.93407600 0.04435800
O 1.20062400 0.96997200 1.29370600
O 2.19304400 0.05105300 -0.43897200
O 0.86098500 1.77360600 -0.72254000
O -1.75590900 2.23020800 0.14942000
H -0.80480600 2.14958400 -0.12221900
H -2.16368900 2.76430300 -0.55668400
O 0.59106200 -1.51563400 -2.08873800
H 0.11471900 -0.96665200 -2.73933600
H 1.24565700 -0.89672800 -1.67401100
O -2.79692900 -0.23988300 0.02416500
H -3.31387500 -0.29069400 -0.80082100
H -2.40492900 0.69100900 0.03187100
O -0.96109500 -1.98276900 -0.07402000
H -0.35990300 -1.78616500 -0.89676100
H -1.71362700 -1.24043800 -0.05050300
H -0.37008800 -1.84750200 0.77271700
O 0.54010100 -1.63845500 1.99196800
H 0.87277200 -0.71112800 1.86202600
H -0.02800300 -1.58889400 2.78330200

$NO_3^-(H_2O)_5(H_3O)^+$
N -0.42496800 -1.72190700 0.33243900
O -0.11976600 -1.99835700 -0.86595400
O 0.47346300 -1.71155200 1.22980600
O -1.62442100 -1.44711500 0.63596400
O -2.75314800 0.08982300 -1.39470500
H -2.41346000 -0.54270600 -0.70946000
H -3.68874900 0.22479200 -1.15728500
O 0.12386200 0.61395100 2.65132300
H -0.80660800 0.70061000 2.93074300
H 0.18026800 -0.29627400 2.25202100
O -1.50001900 2.40248900 -0.86267400
H -1.17948600 2.73039700 -1.72289900
H -1.95705800 1.52670800 -1.07006200

O 0.53159200 2.19664900 0.65804500
H 0.33703900 1.54620000 1.44312300
H -0.30206700 2.22772500 0.02134600
H 1.35292100 1.82650200 0.11720400
O 2.55290800 1.40318400 -0.66387300
H 2.51603600 0.42651000 -0.91703300
H 3.32631200 1.48116700 -0.07541600
O 2.49725400 -1.18195800 -1.37590300
H 2.56737000 -1.19939300 -2.34783300
H 1.58845700 -1.53580800 -1.18774100

$NO_3^-(H_2O)_6(H_3O)^+$
N -0.00874700 0.17749100 -1.70168900
O 1.25800100 0.22373400 -1.72809500
O -0.60267300 -0.93950600 -1.78847100
O -0.68069300 1.24646600 -1.58461100
O 0.73497000 3.14538400 -0.14022400
H 0.27801100 2.50814000 -0.75116900
H 1.48659600 3.48179400 -0.66165100
O -3.08978400 -0.84485700 -0.57469200
H -3.68039800 -0.25166500 -1.07368500
H -2.24263900 -0.84271700 -1.09598800
O 1.76584400 1.43690600 1.65841800
H 1.39142100 2.10095200 0.99653900
H 1.96941100 1.96168600 2.45430200
O -0.00485300 -0.27087900 2.32778100
H 0.70205600 0.44485000 2.03547000
H 0.22765900 -1.18051400 1.86180900
H -0.95271500 0.03808500 2.00502300
O 0.52284600 -2.51070100 1.23328200
H 1.22005800 -2.38762100 0.51386200
H 0.95109100 -3.07101700 1.90627000
O 2.30893600 -2.15237600 -0.74330000
H 3.14915200 -1.87706200 -0.33315800
H 1.95874200 -1.32261700 -1.16444900
O -2.31603600 0.52389100 1.60337600
H -2.93644500 0.28259000 2.31540200
H -2.63322800 0.00816200 0.79552700

$NO_3^-(H_2O)_7(H_3O)^+$
N -2.57201300 0.18677000 0.52495400
O -2.93037500 -1.02517800 0.63739600
O -1.90227200 0.73864700 1.44819500
O -2.87761100 0.84171200 -0.51782100
O -1.12576100 2.96390600 -0.92717700
H -1.77270500 2.23095100 -0.74535600
H -1.30434200 3.21772100 -1.85100500
O 0.35211800 -0.88897400 1.94819000
H 1.06053000 -0.18868900 1.85637300

H -0.49490800 -0.38158800 1.88213700
O 2.32637100 0.94174800 1.45384800
H 1.95151800 1.41830000 0.65570600
H 2.52382200 1.63465600 2.10962300
O 0.62910100 -2.16429700 -0.25402900
H 0.47433600 -1.64973800 0.64880200
H 1.21945800 -1.51873900 -0.86547200
H -0.28971600 -2.29477700 -0.70617800
O 2.09331700 -0.64879400 -1.64083400
H 1.74211100 0.27036900 -1.48295400
H 2.93943000 -0.65648000 -1.10235400
O -1.70425700 -2.55707900 -1.32294800
H -1.74059400 -2.12107500 -2.19453000
H -2.28509100 -2.00203300 -0.74173600
O 4.24616100 -0.46343200 0.04585800
H 4.38597000 -1.32561000 0.47784800
H 3.66638300 0.04054500 0.67838200
O 1.34219700 1.90513600 -0.88151500
H 0.41461400 2.30005600 -0.91367700
H 1.92135600 2.57159200 -1.29359100